Melting of small Sn clusters by *ab initio* molecular dynamics simulations

Feng-chuan Chuang,[1] C. Z. Wang,[1] Serdar Öğüt,[2] James R. Chelikowsky,[3] and K. M. Ho[1]
[1]*Ames Laboratory, U.S. Department of Energy and Department of Physics and Astronomy, Iowa State University, Ames, Iowa 50011, USA*
[2]*Department of Physics, University of Illinois at Chicago, Chicago, Illinois 60607, USA*
[3]*Department of Chemical Engineering and Materials Science, and Minnesota Supercomputing Institute, University of Minnesota, Minneapolis, Minnesota 55455, USA*

(Received 9 September 2003; revised manuscript received 28 January 2004; published 19 April 2004)

Ab initio Langevin molecular dynamics simulations were performed to study the structural transformation of tin clusters Sn_x ($x=6$, 7, 10, and 13) at high temperatures. The melting temperatures of these clusters were estimated to be 1300 K, 2100 K, 2000 K, and 1900 K, respectively, which are all above the melting temperature (505 K) of bulk tin. These results are consistent with recent ion mobility measurements.

DOI: 10.1103/PhysRevB.69.165408 PACS number(s): 36.40.Ei

I. INTRODUCTION

Since early 20th century, it has been realized that higher ratio of number of surface to bulk atoms causes size-dependent melting temperature depression of nanoclusters.[1] This ratio increases as the size of the cluster reduces. According to the simple model proposed by Hanszen, melting temperature of a cluster can be defined as the temperature of equilibrium between a thin liquid layer at the surface of the cluster and the solid sphere core that is embedded in the liquid overlayer.[2] Experimental studies of surface melting on metal clusters[3,4] further validate the assumption that surface atoms contribute to the depression of melting. Nanocalorimetric measurements by Lai *et al.*[4] showed that for copper substrate supported and carbon coated tin clusters with size radii from 50 to 500 Å, the melting temperature is lower than bulk melting temperature and decreases as size of cluster reduces. Bachels *et al.*[5] also observed that melting temperature for tin nanoparticles with radius of 14 Å (around 430 atoms) is lower than the values obtained by Lai *et al.*[4] Two x-ray-diffraction studies of tin nanoclusters[6,7] showed that even supported tin nanoclusters with radii around 25 Å still exhibit melting temperature depression. All the previous studies as discussed above[1,2,4–7] suggest that melting temperature of a cluster is lower than the corresponding bulk melting temperature and decreases as the size of the cluster reduces.

In the extreme case that the size of a cluster is less than the critical radius, all atoms in a small cluster can be considered as surface atoms and there is no bulk atom underneath surface layer. At this regime, surface premelting can be regarded as a melting of whole cluster. One might expect that the same melting temperature depression still exists for tin clusters with radius less than 14 Å. However, recent ion mobility measurements by Shvartsburg and Jarrold[8] showed that tin clusters exhibit prolate geometries and the melting temperature of a tin cluster ion with number of atoms between 10 and 30 is at least 50 K higher than the bulk melting temperature. In the experiment, tin clusters were generated by pulsed laser vaporization of a white tin rod, then cooled down to 78 K. Tin clusters were injected into a temperature-controlled helium tube. Assuming that a tin cluster shall form a perfect liquid droplet once it melts, the melting of the cluster can be monitored by relative ion mobilities defined as the measured mobility divided by the calculated mobility for a hypothetical spherical cluster with the same number of atoms. Therefore, the lower the relative mobility is, the more it deviates from the spherical structure. As the helium tube temperature is raised, they found that the measured ion mobilities did not change up to 555 K for the clusters of 10 to 30 atoms. This provides the evidence that tin clusters still keep the prolate structure and have not changed their shapes dramatically at 555 K.

Lu *et al.*[9] have performed Car-Parrinello *ab initio* molecular dynamics simulations to study the structures of Si, Ge, and Sn clusters with up to 13 atoms. Simulated annealing was performed in order to find the lowest-energy structures. In cooling from high temperatures, mean-square displacement (MSD) as a function of simulation time was plotted in order to identify the structural transformations. It was shown that a transition from high-temperature phase to ground-state structure occurred when no further dramatic change in MSD was observed. Using this criterion, the transition temperatures for the tin clusters containing up to 13 atoms are all above 900 K. Since the simulations were performed by cooling from high-temperature gas and liquid phases, the results of Lu *et al.* suggest that melting temperatures of the tin clusters may be above 900 K.

Very recently, Joshi *et al.*[10,11] performed *ab initio* isokinetic molecular dynamics simulations to study thermal properties of Sn_{10} and Sn_{20} clusters. For the case of Sn_{10}, they concluded that there are two transitions at 500 and 1500 K as the temperature is increased.[10] They noted from the simulations that at 1600 K there were three isomers whereas at 2000 K the number of isomers is as many as 7. By analyzing the atomic trajectories, they found that Sn_{10} cluster retains lowest-energy structure at $T<500$ K, undergoes a permutational rearrangement of atoms that preserves the trigonal prism core of the ground state at $500\ \text{K} \leqslant T \leqslant 1500$, and finally starts to exhibit core distortions and breaks up core at $T>1500$ K which is suggested to be a detectable change in ion mobility experiment. In addition to atomic trajectories, they plotted both the specific heat and root mean square of bond length fluctuation (RMSD) vs temperature. They

showed that there is a turning point at 500 K and a peak at around 2300 K in the specific heat. Neither peak nor shoulder at 1500 K is observed in the specific heat. Moreover, in spite of fluctuation in the plot of RMSD vs temperature, there is a trend of slow increment when the temperature is above 1000 K.

For the case of Sn_{20} clusters, they chose the combined structure of two tricapped trigonal prism (TTP) Sn_{10} as the initial structure.[11] Similar to Sn_{10}, they observed three modes of ionic motion: (i) change in relative orientation of two Sn_{10} units, (ii) an internal rearrangement of ions within TTP unit, observed above 500 K, and (iii) the distortion of at least one TTP unit accompanied by the interchange of atoms between the two TTP units, observed after 800 K. In the plot of the specific heat vs temperature, they showed that there are two peaks at 500 and 1200 K and a small shoulder at 850 K corresponding to transition temperature from mode (ii) to mode (iii). In the plot of RMSD vs temperature, two shock increments are at 650 and 1250 K.

Despite the studies as discussed above, our understanding of the melting of tin clusters is still far from complete. Many interesting questions remain open, such as the dependence of the melting temperature on the size of clusters, atomistic processes of structure isomerization, diffusion as well as melting, and the conceptual connection of cluster melting to melting processes in bulk. Hence, more systematic and quantitative studies on the subject are highly desirable. In this paper, we present an extensive *ab initio* molecular dynamics (MD) simulation study of melting and structural transformation of tin clusters. We develop several criteria for monitoring the structural changes in the clusters during the simulations in order to estimate the melting temperatures of the clusters. Sn_6 (tetragonal bipyramid or octahedron), Sn_7 (pentagonal bipyramid), Sn_{10} (tricapped trigonal prism), and Sn_{13} (from Lu's study) (Ref. 9) were chosen for this study. These four clusters represent three different classes of cluster shapes: Sn_6 and Sn_7 are oblate, Sn_{10} is spherical, and Sn_{13} is prolate. We used Langevin dynamics to simulate tin clusters in a helium tube at different temperatures. Melting temperatures for Sn_6, Sn_7, Sn_{10}, and Sn_{13} were estimated to be about 1300 K, 2100 K, 2000 K, and 1900 K, respectively. These temperatures are all above the melting temperature (505 K) of bulk tin. Simulation results are consistent with recent ion mobility measurements.

This paper is organized as follows. In Sec. II the simulation and analysis methods are described. In Sec. III, simulation results are presented. A discussion of our findings is given in Sec. IV, and the conclusions are drawn in Sec. V.

II. SIMULATION METHODS

Our calculation is based on first-principles density-functional theory within the local-density approximation.[12] The Kohn-Sham equations are solved in real space by the higher-order finite-difference method.[13] Electronic configuration of $5s^2 5p^0 5d^2$ and cutoff radii of 2.5 a.u. for *s*, *p*, and *d* are used to generate Troullier-Martins nonlocal pseudopotentials[14] in Kleinman-Bylander form[15] using *s* as local component. The exchange-correlation term was approximated by Ceperley-Alder functional with Perdew-Zunger parametrization[16]. We used a grid size of 0.5 a.u. and zero boundary conditions requiring the wave functions to vanish 12 a.u. away from outermost atoms of a given cluster. Furthermore, Langevin dynamics is successfully coupled to this higher-order finite-difference method.[17,18] This integration is very efficient for studying localized systems and has been successfully applied to determination of the lowest-energy structures for clusters.[17–21]

Here, we performed isothermal Langevin dynamics[17,18] to simulate the dynamics of the cluster as in ion mobility experiment.[8] In this approach, the atomic positions $\vec{R}_a$ evolve according to Langevin equation

$$M_a \ddot{\vec{R}}_a = \vec{F}_a - \gamma M_a \dot{\vec{R}}_a + \vec{W}_a , \tag{1}$$

where $\vec{F}_a$ is the interatomic force acting on ath atom, M_a is its nuclear mass, γ is the friction coefficient which determines the dissipation rate, and $\vec{W}_a$ are the stochastic forces defined as random Gaussian variables with a white noise spectrum,

$$\langle W_a^{\xi}(t) \rangle = 0,$$

$$\langle W_a^{\xi}(t) W_b^{\xi}(t) \rangle = 2\gamma M_a k_b T_g \delta_{ab} \delta(t-t'),$$

$$\xi = \{x,y,z\}, \tag{2}$$

where T_g is a given temperature and the angular brackets in Eq. (2) denote ensemble or time average. When tin clusters drift in a helium gas tube, helium atoms collide with tin atoms. Tin cluster reaches an equilibrium with the heat bath (helium gas) through these collisions which produce random forces as well as viscous forces on the drifted tin clusters. Since all atoms in a small cluster are surface atoms, we assume all atoms are collided by helium atoms. Here, friction coefficient γ is taken to be 5×10^{-4} a.u. and MD time step is 200 a.u. (4.8 fs, 1 a.u.=0.024 fs). The convergence of potential energy at each MD step is 10^{-3} eV.

Since our purpose is to determine transition temperatures, temperature control for small clusters is one of the key issues in the simulations. For a given simulation temperature T_g, the actual temperature T of the cluster is calculated using two different relations. For a tin cluster with n atoms,

$$\tfrac{3}{2}(n-2)k_B T = \langle E_{kin} - E_{rot} \rangle \tag{3}$$

and

$$\tfrac{3}{2}(n-1)k_B T = \langle E_{kin} \rangle \tag{4}$$

are two relations we used to calculate the temperatures of systems. Additional three degrees of freedom due to the rotation are reduced from the relation in Eq. (3) as compared to Eq. (4). The kinetic energy E_{kin} and the rotation energy E_{rot} are given as follows:

$$E_{kin} = \sum_{i=1}^{n} \frac{1}{2} m_i |\vec{v}_i - \vec{v}_c|^2, \tag{5}$$

where $\vec{v}_i$ is the velocity of ith atom and $\vec{v}_c$ the velocity of center of mass:

$$E_{rot} = \tfrac{1}{2} I \omega^2, \tag{6}$$

where I is the principal moment of inertia and ω is the angular velocity. The average kinetic $\langle E_{kin} \rangle$ and the average rotation energy $\langle E_{rot} \rangle$ are calculated by averaging over all simulation steps at each temperature excluding first 250 MD steps. We verified that the calculated system temperatures using both equations are close to each other within 1% and T is within average $6 \pm 2\%$ of given temperature T_g.

The force acting on atoms is computed by using the Hellman-Feynman theorem.[22] The distribution of electronic states is modeled by Fermi-Dirac statistics with the Fermi temperature set to 300 K. Since energy gaps between HOMO-LUMO (highest occupied molecular orbital–lowest unoccupied molecular orbital) are greater than 0.8 eV (at $T = 0$ K) for all tin clusters studied in this work, very few electrons can be excited above the gap before the melting of the clusters. We further checked the effects of the Fermi temperature on our simulation results at temperature right below transition temperature to ensure that the choice of Fermi temperature in our simulation will not affect our conclusions.

We calculated three different structural properties of the clusters as a function of temperature in order to determine at what temperature tin cluster will change its shape. The first one is root-mean-square deviation of pair distances with respect to ground-state structure as a function of time t:

$$\delta(t) = \frac{2}{n(n-1)} \sum_{i<j} [\langle r_{ij}^2 \rangle_t - r_{ij}^2(0)]^{1/2}, \tag{7}$$

where n is the number of atom in the cluster, $r_{ij}(0)$ is the pair distance of ith and jth atoms at ground-state structure, and $r_{ij}(t)$ is the pair distance of ith and jth atoms at time t. It is clear from Eq. (7) that the higher the value of δ is, the more the cluster deviates from its ground-state structure. The main difference between our definition and that used in previous study in Ref. 10 is that we used the bond length $r_{ij}(0)$ of the ground-state structure (initial structure) rather than the average bond length $\langle r_{ij} \rangle_t$ of whole simulation. The RMSD values calculated from our definition of Eq. (7) tell us how the structure of the cluster deviates from its ground-state structure whereas the RMSD in Ref. 10 gives information about how the structure deviates from its average structure from the simulation. We believe that using ground-state structure as the reference should show more clearly to the structural changes in the clusters than using average bond length as the reference used in Ref. 10.

We use RMSD of pair distances instead of commonly used MSD over atomic positions in order to eliminate the rotational effect caused by Langevin dynamics on the clusters with small number of atoms. Another reason to choose the RMSD is that it could directly relate to Lindemann criterion,[23] which states that a bulk crystal structure will melt when the root-mean-square deviation of bond length of the atoms is more than 10% of the equilibrium bond distance in the crystal. Although clusters are different from the bulk crystalline structure, we will use this criterion as a reference for our present study of cluster melting. Note that our definition of RMSD is referring to all atomic pair distances in the cluster, and the average pair distances of the ground-state structures $r_{ij}(0)$ are 3.26, 3.44, 3.87, and 4.36 Å, for Sn_6, Sn_7, Sn_{10}, and Sn_{13}, respectively. Therefore, we will use 0.326, 0.344, 0.387, and 0.436 Å as the critical RMSD values for Sn_6, Sn_7, Sn_{10}, and Sn_{13}, respectively, in our discussion of the following section. We calculated δ every 100 MD steps (0.48 ps) at different temperatures and plotted δ vs MD steps at different temperatures to see how the δ changes. We also plotted δ vs temperature to determine the transition temperatures.

The second quantity we used to monitor the structure changes in a cluster is based on classical mechanics. The shape of a rigid body is related to the principal moments of inertia of the system. Therefore, distribution of principal moments of inertia at different temperatures can be used to identify the shape changes of the clusters.

Another quantity to measure the structure of the clusters at different temperatures is the radial distribution function $j(r)$. $j(r)$ is defined such that $j(r)dr$ gives the average number of atoms whose distance from a given atom in the cluster is between r and $r+dr$.

We also examined the atomic trajectories (movies) to identify the movements of the atoms and isomer changes during the simulation. We keep track of not only structure but also the index of atoms. Such inspections together with quantitative analyses as discussed above give us a more clear picture about the dynamics of the clusters.

Finally, we also calculated the total energies of the clusters as a function of temperature in order to probe the structural transition in the clusters. For each given temperature T_g, the average temperature T, the average potential energy $\langle E_{pot}(T) \rangle$, and its standard errors are calculated. The total energy of system is given as $\langle E_{total}(T) \rangle = \langle E_{kin}(T) \rangle + \langle E_{pot}(T) \rangle$ at temperature T. In addition, the deviation energy δE is defined as the total energy $\langle E_{total}(T) \rangle$ minus its classical limit $E_0 + 3nk_BT$, where E_0 is the ground-state energy. δE gives the information about how much the potential energy differs from that of the ideal simple harmonic oscillator, and can be used as an indicator for anharmonic effects or structural transformation. We smoothed the plot of δE vs temperature T using five-point moving average method. The error bars in the plots are the standard errors of every five data points

III. RESULTS

A. Sn_6

For Sn_6, the simulations were performed for at least 6000 MD steps at temperatures between 1200 and 2300 K, for 5600 MD steps at 600 K, and for 3300 MD steps at 900 K. The root-mean-square deviation of pair distances δ as a function of simulation time at different temperatures was calculated and plotted in Fig. 1(a). The behavior of δ can be divided into three regimes. Below 1200 K, the plot of δ becomes flat below the level 0.3 Å after around 1000 MD

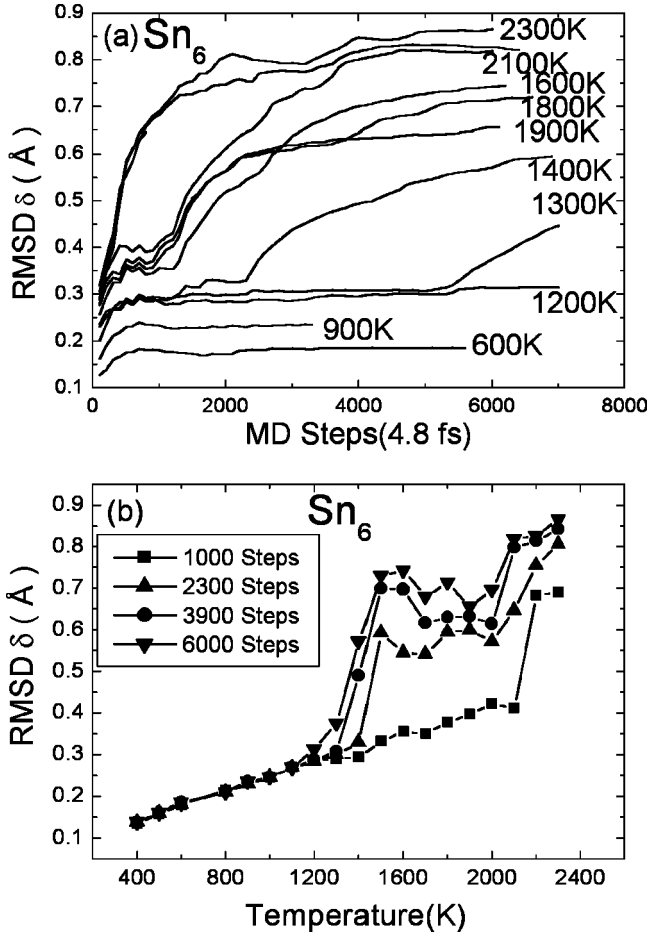

FIG. 1. (a) The RMSD δ of Sn_6 vs MD steps at different temperatures. (b) The RMSD δ of Sn_6 vs temperature at different MD steps as indicated.

steps. At 1300–2100 K, the curve starts out as flat, then exhibits a sudden rise at some critical MD step. At 1300 K, δ is observed to be flat initially, and then starts to rise above the critical value of 0.326 Å (see the discussion in Sec. II) after 5200 MD steps (25 ps), which indicates a structural transition. The plots in Fig. 1(a) show that the higher the temperature of the cluster, the shorter the first flat region tends to be. From 2200 to 2300 K, the plot increases dramatically for a short-time duration, then eventually becomes flat because of the finite size of the cluster.

In Fig. 1(b), we plot RMSD δ as a function of temperature at the moments of 1000, 2300, 3900, and 6000 MD steps, respectively. These data were obtained by intercepting the δ vs MD steps curves in Fig. 1(a) by three vertical lines at 1000, 2300, 3900, and 6000 MD steps, respectively. Because the clusters do not transform to other isomers below 1200 K, we also calculated RMSD for temperatures from 400 to 1200 K with interval of 100 K by performing simulations over 1000 steps (4.8 ps). We found that 1000 steps are adequate for estimating RMSD at these temperatures as one can see from Fig. 1(a) where RMSD becomes almost a constant after about 500 steps at temperatures 600, 900, and 1200 K. From the plots of Figs. 1(a) and 1(b), transition temperature of the system can be estimated using the sudden

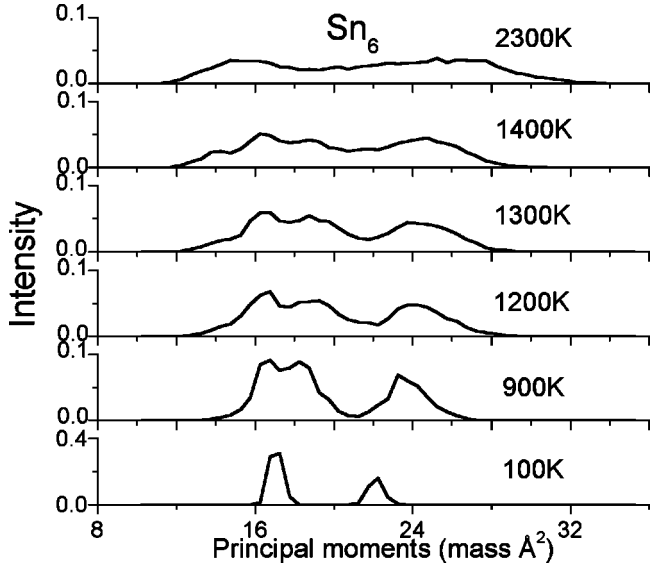

FIG. 2. Distribution of principal moments of inertia of Sn_6 at different temperatures.

increase of δ as an indicator for structural transformation to occur. Transition temperature that we determined from the simulation data at 2300 (11 ps), 3900 (18 ps), and 6000 (28.8 ps) MD steps are 1500, 1400, and 1300 K, respectively. This trend suggests that the transition temperature of the cluster would be lower than 1300 K if the simulations can be performed for longer time. We will discuss this point later in this paper.

Distribution of principal moments of inertia at different temperatures is plotted in Fig. 2. We observed that there were two peaks at lower temperatures and the peaks became broader as temperature increased. The peaks begin to merge at the temperature of 1200 K. Finally, the distribution is almost uniform at a very high temperature of 2300 K. Although it is difficult to determine transition temperature accurately by observing the change in distribution of principal moments, the evolution of the principal moments of inertia with temperature indicates that there is a structural transition around 1300 K which is consistent with the prediction from the analyses of the RMSD δ as discussed above. This is also true in the cases of Sn_7, Sn_{10}, and Sn_{13}.

The radial distribution functions $j(r)$ at different temperatures were also studied. We observed sharp peaks at low temperature and these peaks become broader as temperature increases. $j(r)$ is not sensitive to the structural changes at high temperatures probably because the system size is too small. Therefore, not much information about structural transitions can be obtained from the radial distribution function in case of Sn_6. Similar features are also observed for Sn_7, Sn_{10}, and Sn_{13}.

Examining the atomic trajectories of the cluster at different temperatures, we found that the cluster retained its lowest-energy structure below 1200 K but the amplitudes of oscillations became larger as temperature increased. At 1300 K, we observed that the cluster still retained its shape at first 5300 MD steps (25 ps) but started to change its shape afterward. A new isomer of Sn_6 found at 5476 MD steps at 1300

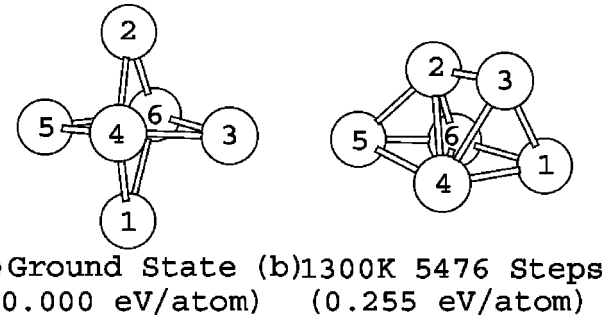

FIG. 3. Sn_6: (a) Ground-state structure, (b) structure of a new isomer at 1300 K. The numbers in parentheses are relative potential energies with respect to that of the lowest-energy isomer.

K is shown in Fig. 3(b). By carefully comparing this structure at 1300 K to the ground-state structure as shown in Fig. 3(a), we could observe the movements of the atoms in the cluster. Specifically, we found that atom 1 moved to the position of atom 3 and pushed atom 3 toward atom 2. At the same time, the bond between atom 1 and atom 5 broke while atom 2 moved more closer to atom 5. The atomic diffusibility in a cluster causes dramatic change in the root-mean-square deviation of pair distances δ. This is consistent with the observation in Fig. 1(a) that a sudden increase in δ at 1300 K is around 5400 MD steps.

The total energy as a function of temperature is plotted in Fig. 4(a). We observed that the curve of total energy could be divided into three regions. The low-temperature region (below 1200 K), transition region ($1200 < T \leqslant 2000$ K), and liquidlike region ($T > 2000$ K). Two solid lines in Fig. 4(a) are obtained by fitting data at low-temperature region and liquidlike region, respectively. By extending the fitted line at low temperatures to higher temperatures as shown by the dotted line, we found that all energy data at the temperature higher than 1300 K are above the extended line. The deviation of total energy of the system from that of the harmonic limit (i.e., $3nk_BT$) as a function of temperature is plotted in Fig. 4(b). The plot shows that there is an increase in energy deviation starting around 1200–1300 K, and reaching a maximum around 2100 K. The results in Figs. 4(a) and 4(b) are consistent with our structural analysis that at 1300 K the structure of Sn_6 starts to change and becomes liquidlike at 2100 K.

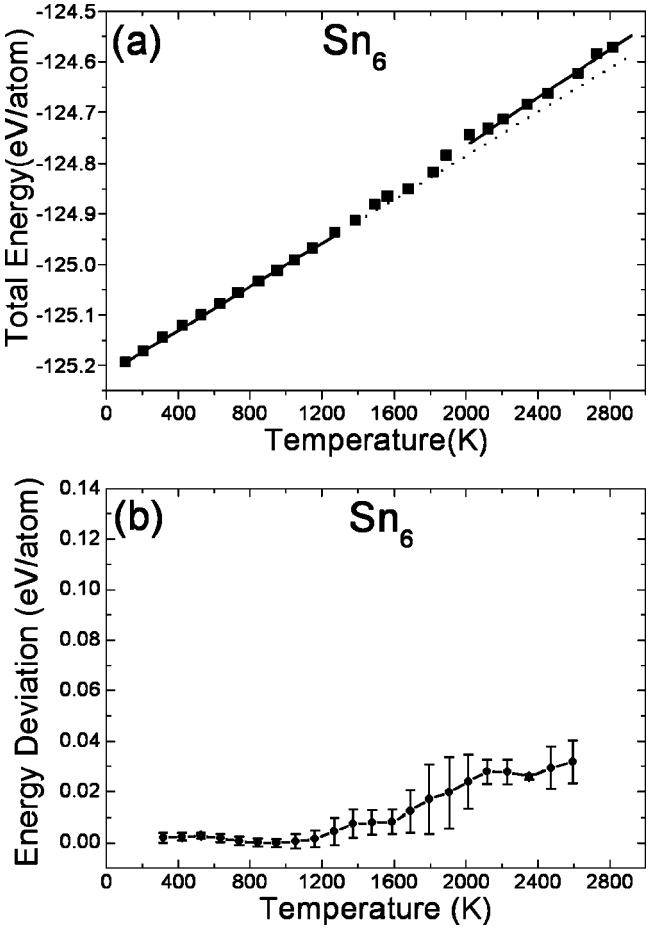

FIG. 4. (a) Total energy of Sn_6 as a function of temperature. The solid lines are obtained by fitting to the data at low-temperature region (below 1200 K) and liquidlike region (above 2000 K). The dotted line is the extension of the low-temperature fitted line to higher temperature. (b) Deviation of total energy of Sn_6 from that of the harmonic limit (i.e., $3nk_BT$) as a function of temperature T. The error bar is the standard error at each temperature T.

B. Sn_7

For Sn_7, the simulations were performed for at least 5600 MD steps at temperatures between 2000 K and 2500 K, for around 1500 MD steps at temperatures from 1600 to 1900 K, and for at least 2300 steps at 500, 600, 1000, and 1500 K. The RMSD δ vs MD steps at different temperatures are plotted in Fig. 5(a). The curves of 2100 and 2200 K were flat in the beginning, and then they started increasing slowly at around 3000 steps, and became flat again in later steps. The values of δ in the first flat region of 2100 and 2200 K are very close to critical value of 0.344 Å. Once the curves start to bend upward, values of δ are greater than 0.344 Å. We notice that at 2100 K, δ started rising earlier than at 2200 K, which is probably due to statistical fluctuations. RMSD δ vs temperature at 1000 (4.8 ps), 3000 (14.4 ps), and 5600 (26.9 ps) MD steps are plotted in Fig. 5(b). From the plots of Fig. 5, a transition temperature is estimated to be about 2100 K for Sn_7.

Distributions of principal moments of inertia at different temperatures are plotted in Fig. 6. We observed that peaks disappeared at 2100 K which indicated that the ground-state structure was no longer retained. In this case, the picture of structural transformation emerging from distribution of the principal moments of inertia is consistent with the plot of δ vs MD steps in Fig. 5(a) and the plot of δ vs temperature in Fig. 5(b).

By examining the atomic trajectories below 2000 K, we found that the cluster retained its lowest-energy structure. However, the structure starts to change at 2100 K. Figure 7(b) shows a new isomer was found at 3152, 4000, and 371 MD steps at 2100, 2200, and 2300 K, respectively. Structural transformation can be seen by comparing this structure with the ground-state structure [Fig. 7(a)]. Specifically, atom 4

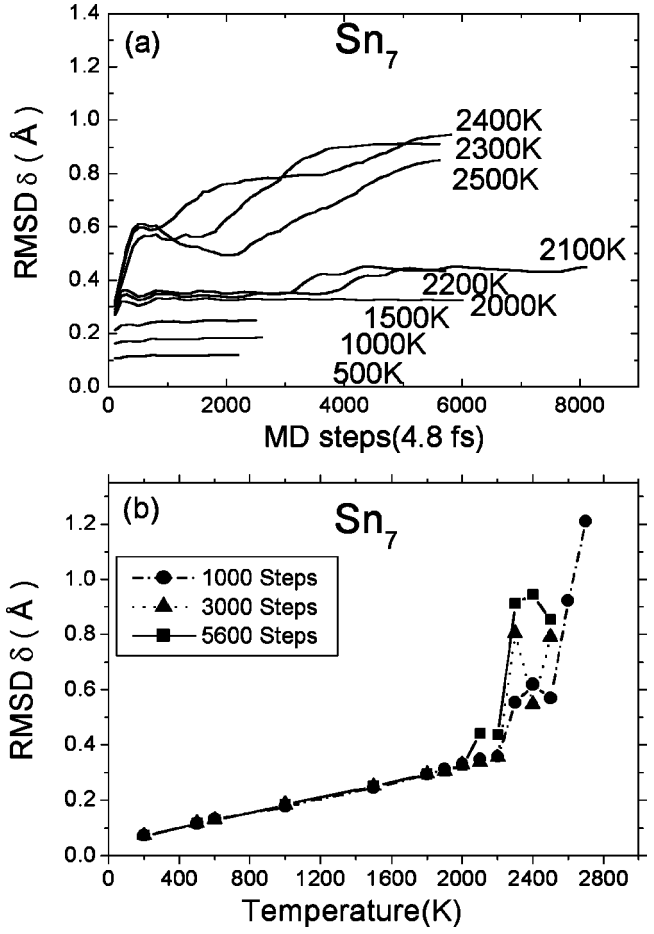

FIG. 5. (a) The RMSD δ of Sn_7 vs MD steps at different temperatures. (b) The RMSD δ of Sn_7 vs temperature at different MD steps as indicated.

moved up to the position of atom 3 and caused a series of diffusions. This diffusive activity is consistent with the plots of δ (Fig. 5) and distribution of principal moments of inertia (Fig. 6).

Finally, the total energy as a function of temperature is plotted in Fig. 8(a). The solid line in Fig. 8(a) is obtained by fitting data at low-temperature region (below 2000 K). We also extended the fitting line at low temperatures to higher temperatures as shown by the dotted line. All data points above 2000 K are found to be located above the extended line. The plot energy deviation vs temperature as shown in Fig. 8(b) showed that there is a shape increase in δE around 2000 K which agrees well with the result of RMSD δ plot in Fig. 5. In contrast to δE plot for Sn_6, no flat region was found in δE for Sn_7 at the high-temperature region. This is because the liquid state is not well developed for Sn_7 even at temperatures as high as 2400 K. The transition we observed at about 2100 K is the isomerization transition. Therefore, the melting temperature of Sn_7 would be above 2100 K. Since we are interested in low bound of melting temperature, the simulations for Sn_7 are sufficient.

C. Sn_{10}

For Sn_{10}, the simulations were performed for at least 4700 MD steps at temperatures between 800–1600 and 2300

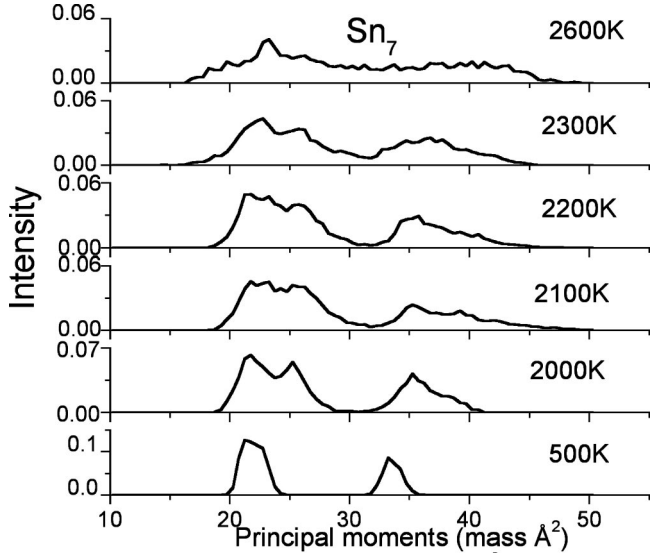

FIG. 6. Distribution of principal moments of inertia of Sn_7 at different temperatures.

K, for 4000 MD steps at 400 and 500 K, and for 2000 MD steps at 100 and 200 K. The root-mean-square deviation of pair distances δ vs MD steps at different temperatures are plotted in Fig. 9(a). We observed that the first structural change occurs at 500 K. Below 500 K the curves are flat. At 500 K, the curve had a short flat part before increasing and became flat again. At 900 K after 3300 MD steps (15.8 ps), we noticed that the curve started to bend upward and passed the critical value of 0.387 Å. This suggests there may be a transition at 900 K. Between 900 and 1400 K, the trends of the plots are similar but with some fluctuations. Above 1400 K the curves increased continuously. The root-mean-square deviation of pair distances δ vs temperature at 2300 (11 ps), 3000 (14.4 ps), and 4700 (22.5 ps) MD steps is plotted in Fig. 9(b). We observe two abrupt changes at 500 and 1400 K. A notable peak of δ at 1200 K in the plot of 4700 MD steps and steady increasing region after 1400 K is observed. The plots of δ vs MD steps and temperature suggested that local

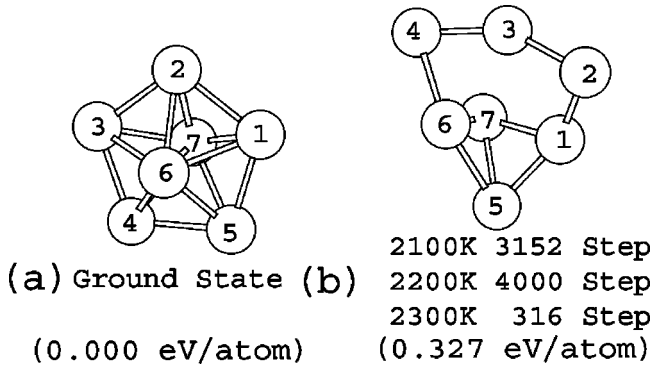

FIG. 7. Sn_7: (a) Ground-state structure, (b) a common isomer found at different temperatures. The numbers in parentheses are relative potential energies with respect to that of the lowest-energy isomer.

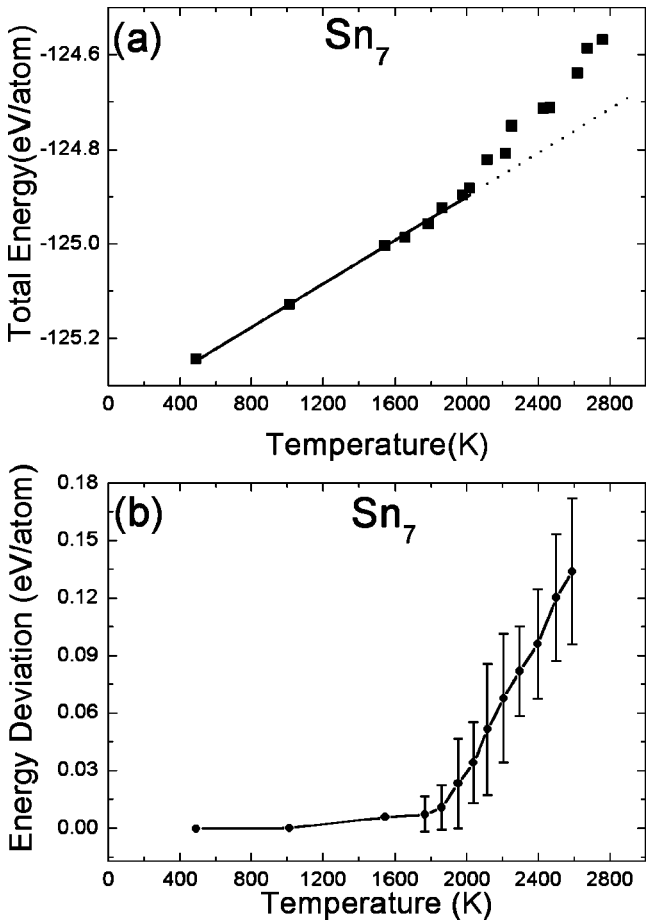

FIG. 8. (a) Total energy of Sn_7 as a function of temperature. The solid lines are obtained by fitting to the data at low-temperature region (below 2000 K). The dotted line is the extension of the low-temperature fitted line to higher temperature. (b) Deviation of total energy of Sn_7 from that of the harmonic limit (i.e., $3nk_BT$) as the function of temperature T. The error bar is the standard error at each temperature T.

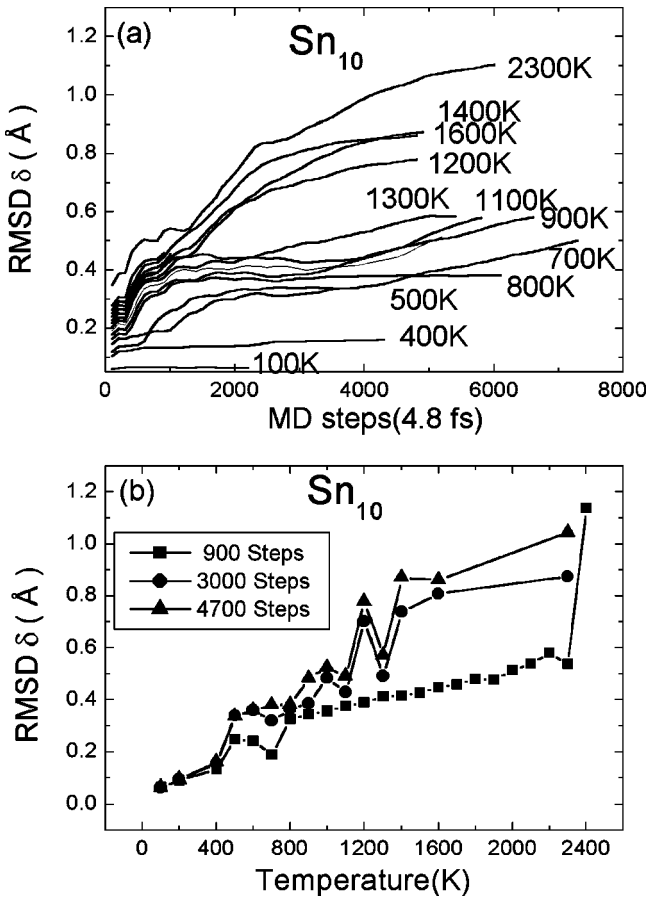

FIG. 9. (a) The RMSD δ of Sn_{10} vs MD steps at different temperatures. (b) The RMSD δ of Sn_{10} vs temperature at different MD steps as indicated.

distortion happens at 500 K, diffusions start to occur at 900 K, and the cluster becomes liquidlike after 1400 K. The fluctuation of RMSD between 500 and 1400 K is also observed in Joshi's study.[10]

Distribution of principal moments of inertia at different temperatures is plotted in Fig. 10. The lowest-energy structure of Sn_{10} is close to a compact spherical structure as shown in Fig. 11(a). Hence, two peaks in distribution of principal moments of inertia at low temperature are close to each other. As temperature increases above 400 K, the distribution becomes a single peak which looks like a normal distribution with different variances at different temperatures. It is interesting to note that at 2300 K the distribution is very broad. This indicates that at such high temperature the cluster tends to break up and the fluctuation in the shape of the cluster is very large. Because of the nearly compact spherical structure of Sn_{10}, the structural transitions are not clearly seen in distribution of principal moments of inertia.

The atomic trajectories collected during the simulations show that below 500 K Sn_{10} cluster retained its lowest-energy structure and atoms moved and oscillated around

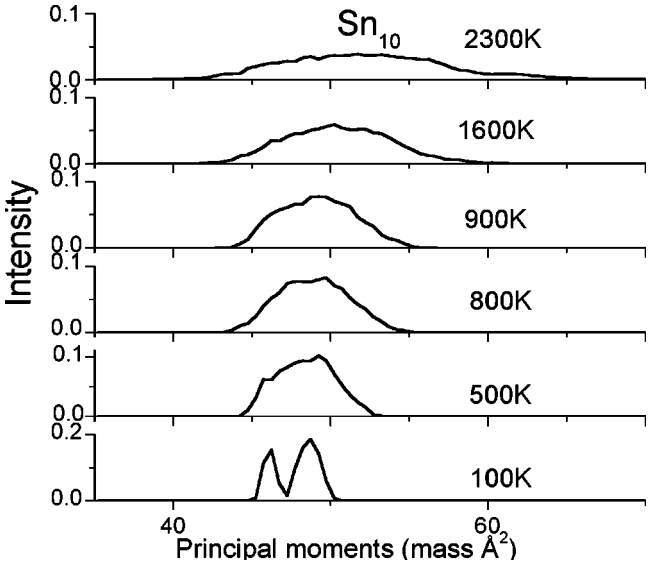

FIG. 10. Distribution of principal moments of inertia of Sn_{10} at different temperatures.

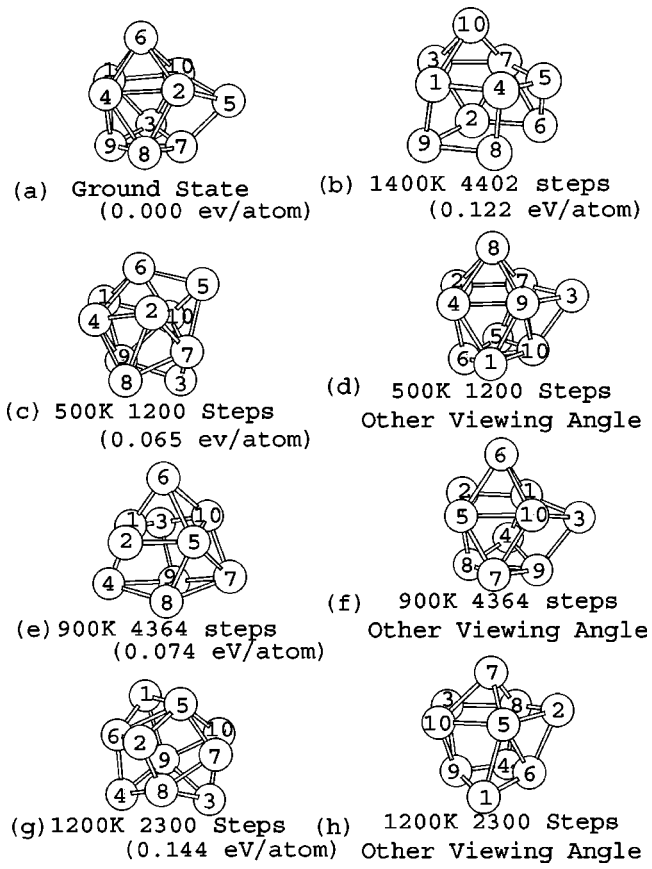

FIG. 11. Sn_{10}: (a) is the ground-state sturcture; (b) is an isomer at 1400 K; (c) and (d) are the same isomer at 500 K; (e) and (f) are the same isomer at 900 K; (g) and (h) are the same isomer at 1200 K. The numbers in parentheses are relative potential energies with respect to that of the lowest-energy isomer.

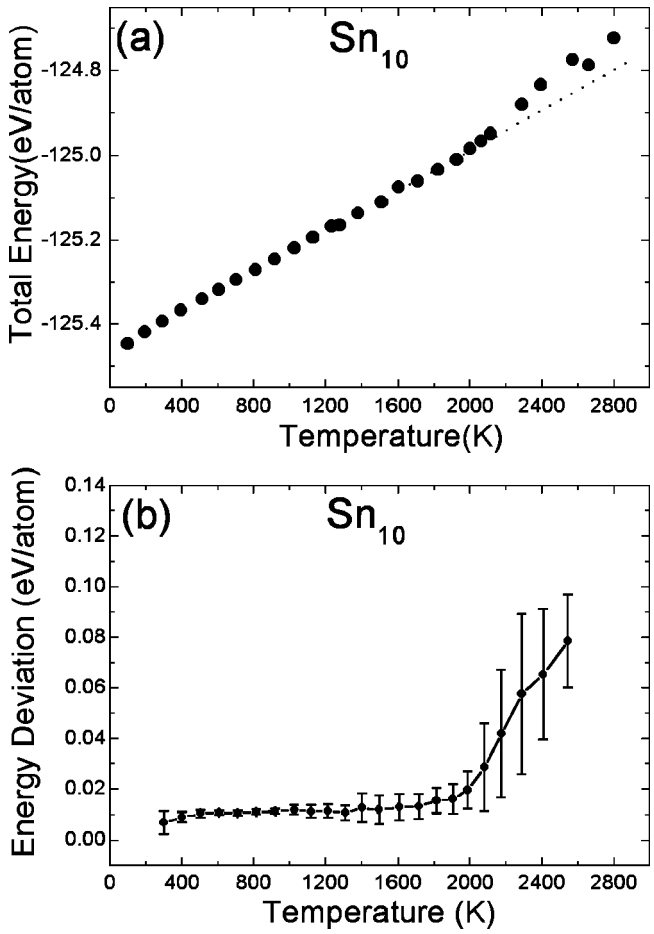

FIG. 12. (a) The solid line is obtained by fitting data at low-temperature region. The dotted line is the extended fitting line of low temperature to higher temperature. (b) Deviation of total energy of Sn_{10} from that of the harmonic limit (i.e., $3nk_BT$) as a function of temperature, after smoothing, where error bar is the standard error at each temperature T.

equilibrium positions. At 500 K cluster started to have obvious distortions. Such distortions seem to change the shape of the cluster if the cluster is viewed from the original direction. However, the structure of the cluster is in fact retained if viewed from a different angle. As shown in Fig. 11, the cluster at 500 K and 1200 steps as shown in Fig. 11(c) looks different from its ground-state structure of Fig. 11(a). However, a structure similar to that of ground-state structure can be seen from the same atomic coordinates but from a different viewing angle as shown in Fig. 11(d). This is because the structure of Sn_{10} cluster is pretty symmetric and the fluctuations of the atomic positions make the cluster switch back and forth between different degenerate configurations. Therefore, we may classify such changes as the first transition (but not the melting transition). Figure 11(e) shows a snapshot taken at 900 K and at the MD step of 4364. We observed that the relative positions of atoms were changed and atoms were able to diffuse in the cluster as shown in Fig. 11(e). This diffusion caused additional increment in the root-mean-square deviation of pair distances δ as we have already noticed at 900 K in Fig. 11(a). Surprisingly, the ground-state structure is still kept if viewed from a different angle as shown in Fig. 11(f). At 1200 K, the atoms are observed to diffuse in a way similar to that at 900 K and the diffusion does not result in any new structures as one can see from Figs. 11(g) and 11(h). However, the diffusion process is much faster at 1200 K as compared to that at 900 K. From experience with Sn_6, such diffusive behavior might also occur at temperatures between 600 and 900 K. The isomer at 1400 K is shown in Fig. 11(b). It seems that the shape is still similar to ground-state structure. However, the relative positions of atoms have changed.

The total energy as a function of temperature is plotted in Fig. 12(a). The solid line in Fig. 12(a) is obtained by fitting data at low-temperature region (below 1600 K). We extended the fitting line at low temperatures to higher temperatures as shown by the dotted line. The plot of energy deviation vs temperature in Fig. 12(b) shows that there is a small increase at 1400 K and a shape increase starts at 2000 K. Between 900 and 2000 K, atoms undergo small diffusive motions. The temperature of 2000 K can be identified as melting temperature from our present simulation. No flat region in δE at the high-temperature region is observed due to the similar reason as we discussed for Sn_7.

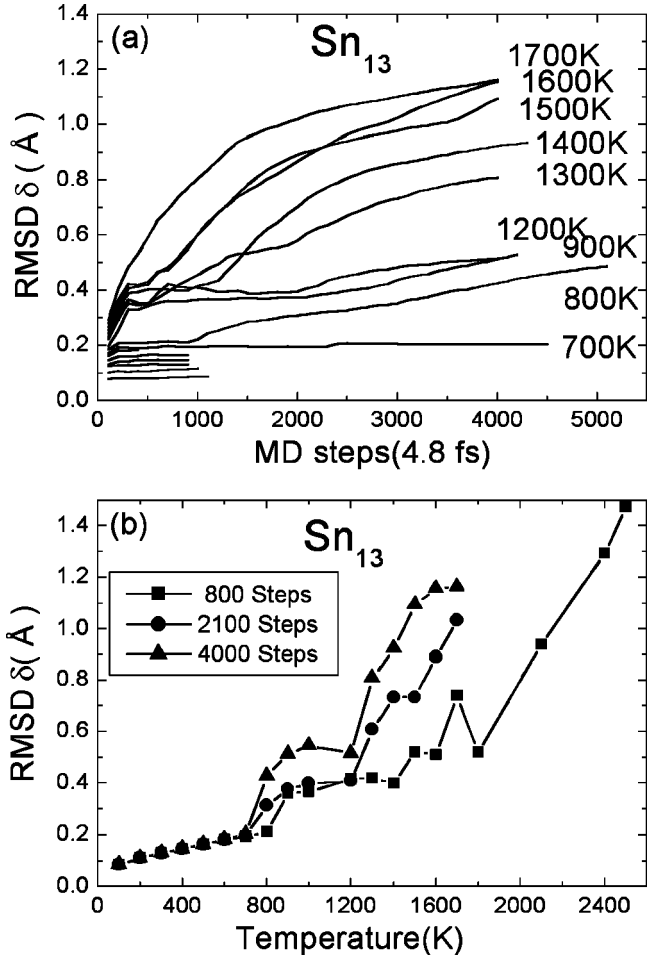

FIG. 13. (a) The RMSD δ of Sn_{13} vs MD steps at different temperatures. (b) The RMSD δ of Sn_{13} vs temperature at different MD steps as indicated.

D. Sn_{13}

For Sn_{13}, the simulations were performed for 4000–5000 MD steps at temperatures between 800 K and 1700 K and for around 1000 MD steps at the rest of the temperatures. The root-mean-square deviation of pair distances δ vs MD steps at different temperatures and δ vs temperature at different MD steps is plotted in Fig. 13. We noticed that the plot of δ at 700 K was flat. At 800 K, δ starts to increase at around 1000 MD steps (4.8 ps). As the simulation continued, RMSD δ continued to increase gradually. We observed that at around 3500 MD steps (16.8 ps) the value RMSD δ crossed over the value of 0.36 Å, but was still smaller than the critical value of 0.436 Å. This variation of δ as a function of time suggests that cluster isomerization starts to take place at the temperature of 800 K. This diffusive dynamics takes place faster when temperature is increased, e.g., from 900 to 1200 K. At 1300–1600 K, the root-mean-square deviation of pair distances δ starts as flat then increases sharply, indicating that the cluster is in a liquidlike state. From 1700 K to 2400 K, the plot of δ increases dramatically in a short period of time indicating that the system is liquidlike after 1700 K. The increase associated with structural change at 800 and 1300 K can be seen from Fig. 13(b).

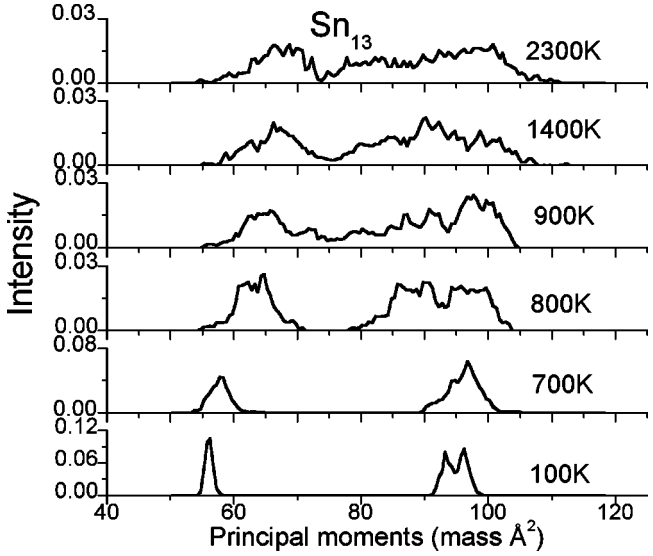

FIG. 14. Distribution of principal moments of inertia of Sn_{13} at different temperatures.

Distribution of principal moments of inertia is plotted in Fig. 14. We observed that two peaks are separated far from each other at low temperatures due to the prolate shape of the cluster. At 800 K the peaks become closer as well as broader. This indicates that prolate structure of Sn_{13} becomes a less prolate one above 800 K. The two peaks become broader and merge together at higher temperature of 1400 and 2300 K. The behavior of the distribution of the principal moment is consistent with that of the RMSD δ.

The atomic trajectories from the MD simulators show that below 700 K atoms move around equilibrium positions and retain its lowest-energy structure. At 800 K, from 1000 to 3700 MD steps, atom 2 that was on top of cluster moved down and pushed atom 10. Atom 10 moved forward and backward between middle level as shown in Figs. 15(a) and 15(c). This corresponds to the shift of distribution of principal moments of inertia at 800 K shown in Fig. 14. At 4026 MD steps, the cluster distorts and starts to change its shape by bending the upper half of the cluster as shown in Fig. 15(d). Hence, we can say that atoms in the upper half start to change their relative positions at 800 K. At 900 K, from 1000 to 2300 MD steps, structure of cluster exhibits similar dynamics at 800 K as shown in Fig. 15(e). After 2300 steps (11 ps), another type of isomerization was observed. Snapshot taken at 3933 steps (18.7 ps) at 900 K is shown in Fig. 15(f). We observed that the cluster changed its shape as follows: Atom 5 in middle layer went to lower layer and atoms 13 and 12 moved toward atom 4. Atom 4 moved from the lower layer up to the middle layer. Shape at 4355 MD steps at 1400 K is shown in Fig. 15(b). One atom in the center of the structure and the relative positions of atoms changed. We notice that the relative potential energy of this isomer is lower than those of isomers at 800 and 900 K.

The total energy as a function of temperature is plotted in Fig. 16(a). The solid lines in Fig. 16(a) are obtained by fitting data at low-temperature region (below 1600 K) and liquidlike region (above 1900 K). We extended the fitted line at

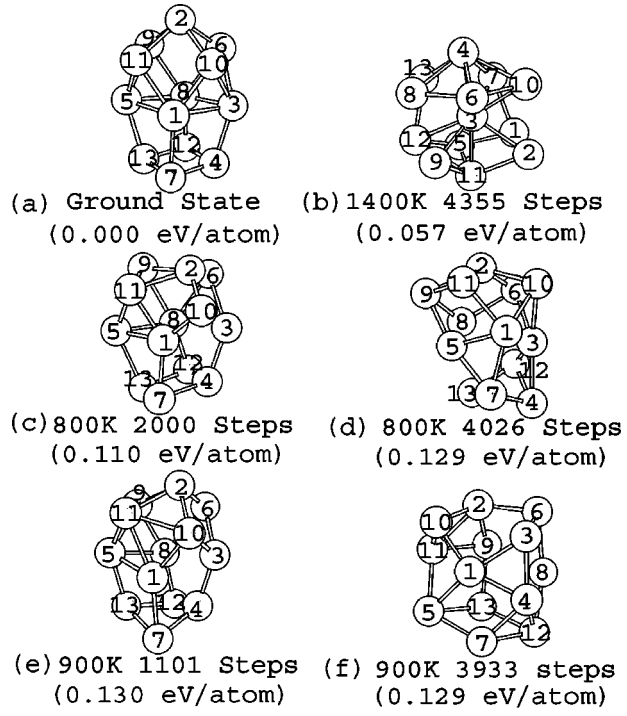

FIG. 15. Sn_{13}: (a) Ground-state structure; (b) an isomer at 1700 K; (c) and (d) are isomers at 800 K; (e) and (f) are isomers at 900 K. The numbers in parentheses are relative potential energies with respect to that of the lowest-energy isomer.

low temperatures to higher temperatures as shown by the dotted line. The energy deviation vs temperature plotted in Fig. 16(b) shows that the big peak starts at about 1600 K and peaks around 2100 K. These results together with the structural information discussed above suggest that the melting transition is at 1800–1900 K.

IV. DISCUSSION

Our simulations show that two types of dynamics may cause the early dramatic changes in the root-mean-square deviation of pair distances δ before it reaches a finite value when the cluster is in a liquidlike region. One is isomerization of the cluster where distortions cause the cluster to transform to a metastable structure before melting. Such isomerization processes contribute only very subtle change to ion mobility. The other is due to the melting transition where substantial atomic diffusion in the cluster is observed. Such diffusion will cause notable change in ion mobility. The change in the RMSD δ is therefore a good indicator of structural transition in a cluster which also can be probed by ion mobility measurement. Here, we define the melting temperature of a cluster as the temperature at which substantial atomic diffusions take place in the cluster. The temperature defined in this way should be the lower bound to the melting temperature. In the cases of Sn_6 and Sn_7, we found melting temperatures are 1300 and 2100 K, respectively. In the case of Sn_{10} and Sn_{13}, although we found structural distortions occurred at 500 and 800 K, and the first diffusion of atoms

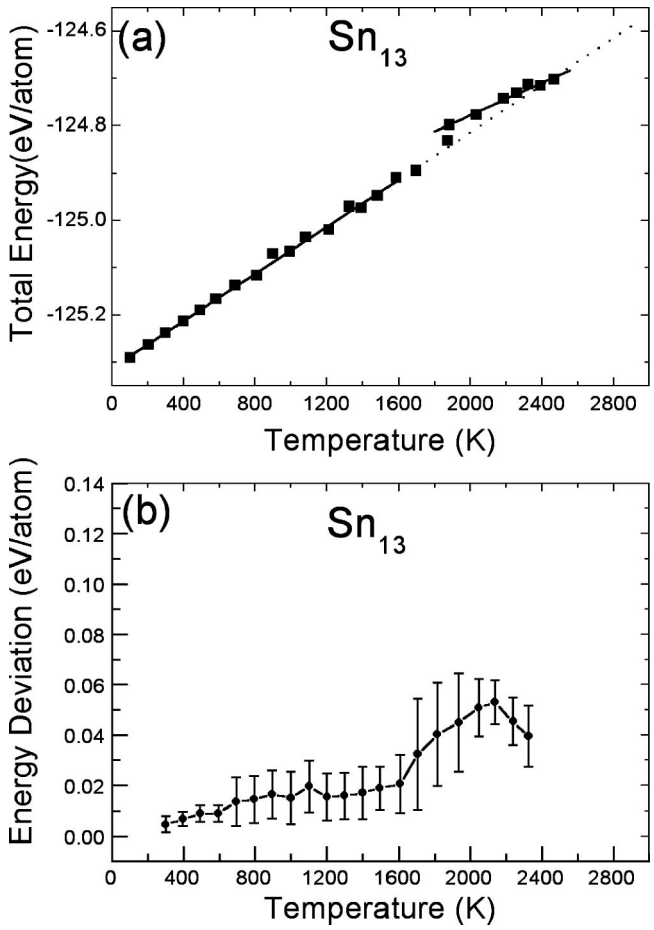

FIG. 16. (a) Total energy of Sn_7 as a function of temperature. The solid lines are obtained by fitting to the data at low-temperature region (below 1600 K). The dotted line is the extension of the low-temperature fitted line to higher temperature. (b) Deviation of total energy of Sn_{13} from that of the harmonic limit (i.e., $3nk_BT$) as a function of temperature T. The error bar is the standard error at each temperature T.

occurred at 900 and 800 K, respectively, the most significant transitions (melting) to the liquidlike state do not occur until 2000 and 1900 K. These results indicate that the melting temperatures of all these clusters are much higher than the Sn bulk melting temperature of 505 K. There is no obvious size correlation to melting temperatures from our present results on the four clusters. The structure and dynamics of tin clusters (Sn_4-Sn_{13}) upon cooling from high-temperature gas phase have been studied by Lu *et al.* using Car-Parrinello molecular dynamics simulations.[9] The results from their simulations also suggest higher melting temperatures for the small Sn clusters.

The molecular dynamics simulations enable us to observe the atomic dynamics of small tin clusters during the heating process. Each atom in the cluster starts with a small local vibration and distortion (stage I). As temperature rises, the amplitudes of the thermal motion increase (stage II). These increasing local distortions may sometimes cause partial isomerization of the clusters if the energy barrier between different local minimum structures is not very high. Both stages I and II are regarded as the solid state. In the case of

Sn_6 and Sn_7, because the energy barriers between the ground state and other metastable states are very high, we did not observe isomerization of these clusters until very high temperatures (1300 and 2100 K, respectively) where the diffusion dynamics dominated. In the case of Sn_{10}, the local fluctuation at 500 K switches the cluster back and forth among several energetically degenerate (global minimum) isomers as shown in Fig. 11. In the case of Sn_{13}, local distortions at 800 K enable the cluster to switch between different metastable structures that look similar to ground-state structure. As temperature continues to rise, big distortions cause some atoms to be pushed to nearby positions which induces a series of correlated diffusions (stage III). Consecutive jumps of atoms in the clusters are often observed when such diffusion takes place. The correlated diffusion induced rapid isomerization of the clusters eventually leads to fully melting of the clusters (liquid state). The dynamics of the clusters upon heating is similar to that observed in the MD simulation of Joshi *et al.* where Sn_{10} has been studied.[10] Moreover, the temperature for stage III to occur was estimated by Joshi *et al.* to be 1600 K which agrees with the results from our studies.

Ion mobility measurement has been used as an experimental probe to investigate the melting of Sn clusters. It is assumed that the clusters will change their shape (toward a spherical shape) upon melting, and the changes can be detected by the measurement of their ion mobility. Our simulation results show that changes to the shape of the clusters may be very small if the ground-state structure of the clusters is already in a spherical shape. For example, from a macroscopic viewpoint, Sn_{10} would not significantly change its shape until 2000 K, although the diffusive dynamics of the cluster has already been noticed at 900 K. On the other hand, we believe that Sn_{13} would start to change its ion mobility significantly above 1300 K and reach a maximum beyond 1900 K according to our simulation.

There is a possibility that the melting temperatures (or the isomerization temperatures) of the clusters are overestimated due to the finite simulation time. Using the simulation results for Sn_6 at different temperatures, we can get a rough estimation of the error in the melting temperature due to the finite simulation time from the following relation:

$$t = t_0^* e^{(E_a/k_B T)}, \tag{8}$$

where t is the duration time of a given structure (i.e., the average time between each diffusion event), E_a is the activation energy, and t_0 is a prefactor (constant). Using the data points from 1300 to 1800 K, we can determine $E_a = 0.875$ eV and $t_0 = 1.93$ MD step by fitting to the above relation as shown in Fig. 17. According to these parameters, 9164 MD steps (44 ps) would be needed to observed one diffusion event at 1200 K, and 19 786 MD steps (95 ps) is needed at 1100 K. Interpolating to lower temperature as shown in the inset of Fig. 17 indicates that the probability of the cluster isomerization is very small when the temperature is lower than 800 K. This supports our conclusion that the melting temperature of Sn_6 cluster is much higher than that of the bulk crystal.

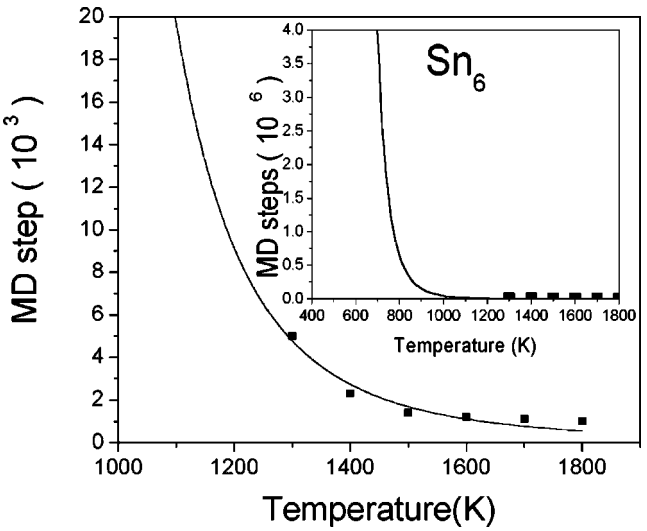

FIG. 17. The lifetimes (MD steps) of Sn_6 at different temperatures are fitted to Eq. (8). The constant t and E are estimated from the fitting. The inset shows interpolation to lower temperature (see text).

V. CONCLUSION

We have performed *ab initio* Langevin dynamics simulations at different temperatures to study the isomerization and melting of small tin clusters. Through the analysis of the root-mean-square deviation of pair distances δ, energies, and the atomic trajectories from the MD simulations, we have determined transition temperatures for the isomerization and melting of the clusters.

In our study of heating up small tin clusters, we successfully divided the structural dynamics of the clusters into three stages before the clusters fully melt. In stage I, atoms vibrate around equilibrium position. In stage II, cluster has distortions but relative positions are preserved. In stage III, some atoms start to diffuse and relative positions of atoms are changed. Once most of atoms diffuse inside clusters, the clusters melt. It is difficult to determine transition between stages I and II for clusters with very few atoms, Sn_6 and Sn_7, because vibration and distortion are strongly coupled for these cases. For Sn_{10} and Sn_{13}, the change from stage I to stage II takes place around 500 and 800 K, respectively. We also found that the temperatures for transition from stage II to stage III are 1300, 2100, 1400, and 1300 K, respectively, for Sn_6, Sn_7, Sn_{10}, and Sn_{13}. The melting temperatures for these clusters are 1300, 2100, 2000, and 1900 K, respectively. These transition temperatures between the solid state to the fully developed liquid state are all higher than melting temperature of bulk tin.

ACKNOWLEDGMENTS

Ames Laboratory is operated for U.S. Department of Energy by Iowa State University under Contract No.

W-7405-Eng-82. This work was supported by the Director of Energy Research, Office of Basic Energy Sciences including a grant of computer time at the National Energy Research Supercomputing Center (NERSC) in Berkeley. One of us (J.R.C.) wishes to acknowledge support from the National Science Foundation, the Computational Materials Science Network (CMSN) of the Department of Energy, and the Minnesota Supercomputing Institute.

[1] P. Pawlow, Z. Phys. Chem. (Leipzig) **65**, 1 (1909).
[2] K.-J. Hanszen, Z. Phys. **157**, 523 (1960).
[3] Z.B. Güvenç and J. Jellinek, Z. Phys. D: At., Mol. Clusters **26**, 304 (1993); R. Garrigos, P. Cheyssac, and R. Kofman, *ibid.* **12**, 497 (1989).
[4] S.L. Lai, J.Y. Guo, V. Petrova, G. Ramanath, and L.H. Allen, Phys. Rev. Lett. **77**, 99 (1996).
[5] T. Bachels, H.-J. Guntherodt, and R. Schafer, Phys. Rev. Lett. **85**, 1250 (2000); R. Kofman, P. Cheyssac, and F. Celestini, *ibid.* **86**, 1388 (2001).
[6] C.E. Bottani, A. Li Bassi, B.K. Tanner, A. Stella, P. Tognini, P. Cheyssac, and R. Kofman, Phys. Rev. B **59**, 15 601 (1999).
[7] L.E. Depero, E. Bontempi, L. Sangaletti, and S. Pagliara, J. Chem. Phys. **118**, 1400 (2003).
[8] A.A. Shvartsburg and M.F. Jarrold, Phys. Rev. Lett. **85**, 2530 (2000).
[9] Z.Y. Lu, C.Z. Wang, and K.M. Ho, Phys. Rev. B **61**, 2329 (2000).
[10] K. Joshi, D.G. Kanhere, and S.A. Blundell, Phys. Rev. B **66**, 155329 (2002).
[11] K. Joshi, D.G. Kanhere, and S.A. Blundell, Phys. Rev. B **67**, 235413 (2003).
[12] P. Hohenberg and W. Kohn, Phys. Rev. **136**, B864 (1964); W. Kohn and L.J. Sham, Phys. Rev. **140**, A1135 (1965).
[13] J.R. Chelikowsky, N. Troullier, K. Wu, and Y. Saad, Phys. Rev. B **50**, 11 355 (1994); J.R. Chelikowsky, N. Troullier, X. Jing, D. Dean, N. Binggeli, K. Wu, and Y. Saad, Comput. Phys. Commun. **85**, 325 (1995); Y. Saad, A. Stathopoulos, J.R. Chelikowsky, K. Wu, and S. Öğüt, BIT **36**, 63 (1996).
[14] N. Troullier and J. L Martins, Phys. Rev. B **43**, 1993 (1991).
[15] L. Kleinman and D.M. Bylander, Phys. Rev. Lett. **48**, 1425 (1982).
[16] D.M. Ceperley and B.J. Alder, Phys. Rev. Lett. **45**, 566 (1980); J.P. Perdew and A. Zunger, Phys. Rev. B **23**, 5048 (1981).
[17] N. Binggeli, J.L. Martins, and J.R. Chelikowsky, Phys. Rev. Lett. **68**, 2956 (1992).
[18] X. Jing, N. Troullier, D. Dean, N. Binggeli, J.R. Chelikowsky, K. Wu, and Y. Saad, Phys. Rev. B **50**, 12 234 (1994).
[19] J.R. Chelikowsky, S. Öğüt, X. Jing, K. Wu, A. Stathopoulos, and Y. Saad, in *Materials Theory, Simulations and Parallel Algorithms*, edited by E. Kaxiras, J. Joannopoulos, P. Vashishta, and R. K. Kalia, Mater. Res. Soc. Symp. Proc. 408 (Materials Research Society, Pittsburgh, 1996).
[20] S. Öğüt and J.R. Chelikowsky, Phys. Rev. B **55**, R4914 (1997).
[21] L. Kronik, I. Vasiliev, and J.R. Chelikowsky, Phys. Rev. B **62**, 9992 (2000).
[22] H. Hellman, *Einfuhrung in Quantenchemie* (Deuticke, Leipzig, 1937); R.P. Feynman, Phys. Rev. **56**, 340 (1939).
[23] F.A. Lindemann, Phys. Z. **11**, 609 (1910).